Please cite publisher's version:

J. McCubbing, P. Murphy, H. Eswaran, H. Preissl, T. Yee, S. E. Robinson and J. Vrba, (2007):
Validation of the flash-evoked response from fetal MEG;
Published in: Physics in Medicine and Biology, 52 5803-5813
http://www.iop.org/EJ/abstract/0031-9155/52/19/005
DOI: 10.1088/0031-9155/52/19/005

Validation of the flash-evoked response from fetal MEG

J. McCubbin, P. Murphy, H. Eswaran, H. Preissl, T. Yee, S. E. Robinson and J. Vrba

Abstract
Flash-evoked responses can be recorded from the fetus *in utero*. However, a standard analysis approach based on orthogonal projection (OP) to attenuate maternal and fetal cardiac signals leads to a spatial redistribution of the signal. This effect prevents the correlation of source location with a known fetal head location in some cases and the signal-to-noise ratio (SNR) is sometimes limited such that the response latency is difficult to determine. We used a modified beamformer model search analysis to avoid the redistribution shortcoming and to improve the SNR. We included a statistical test for residual interference in the average and quantified significance of the evoked response with a bootstrap method. Selected source locations compared favorably to fetal head locations estimated from ultrasound exams. The evoked response time course was found to have a significant post-trigger peak with a latency between about 180 and 770 ms in more than 90% of the subject measurements. These results confirm that the combined application of a beamformer model search and bootstrap significance test provides a validation of the flash-evoked response observed in OP processed fetal MEG channels.

1. Introduction

The investigation of fetal brain development *in utero* in humans can be performed by fetal magnetoencephalography (fMEG). There is growing evidence that fMEG is able to detect auditory-evoked responses, flash-evoked responses and spontaneous brain activity. The investigation of flash-evoked responses is especially interesting, because the stimulation is not perceived by the mother; avoiding a potential event-related artifact. Validation of the fetal averaged evoked response is complicated by a poor SNR due to the presence of fetal

spontaneous brain activity, fetal eye and mouth movements and unidentified interferers within the maternal abdomen which may not be sufficiently attenuated by the limited number of averaged events. The problem is exacerbated at this point in the development of fMEG due to the absence of co-registration between the MEG sensor array and a 3D ultrasound image of the fetus. The low SNR regime suggests that validation of these results should include (a) statistical significance of the time course, (b) proximity of significant MEG sensor channels (or a modeled source) to the estimated fetal head location and (c) observation of physiologically plausible time course morphology.

In our initial report of flash-evoked fMEG (Eswaran *et al* 2002) we observed an evoked field in only 63% of the cases. However, we have recently reported an improved response using orthogonal projection (OP) processing (McCubbin *et al* 2007a). The improvement over prior efforts, observed as an increase in the number of successful recordings from 63% to 89%, was attributed to an upgraded visual stimulator, better measurement protocol and processing advancements.

A significance measure was applied in the recent work, using the pre-stimulus interval for estimation of the background noise in the average. However, e.g. in cases with large spontaneous burst brain activity often seen in the late gestation fetus (Rose and Eswaran 2004), the pre-stimulus interval available for the estimation of the statistical distribution for the background interference may not be sufficient to conservatively satisfy the significance validation (a). The redistribution of the fMEG signal among MEG channels due to OP processing (Vrba *et al* 2004) made it difficult to carry out the proximity validation (b), however the morphology criterion (c) was qualitatively successful.

An alternate approach would be to fit a dipole model to the OP processed and averaged time course and then project the modeled dipole activity back to the MEG sensor space. This could eliminate the proximity validation difficulties, but does not provide any benefit in SNR for the other validation criteria. In the current work we investigated a beamformer model search (Vrba *et al* 2007) to improve SNR over the OP processing method and to allow correlation of the selected fetal head model to the estimated fetal orientation. In addition the beamformer approach suppresses environmental interference and other interfering sources which cannot be identified by template matching for OP. The beamformer applies a spatial filter which attenuates all signal components that do not support a modeled source at the target location and provides a transformation of the MEG signal space to a single source activation. Beamformer rejection of MCG is superior to that obtained with OP and it additionally attenuates other interference arising from sources external to the fetal head. The beamformer is well suited to situations where the source model is not well known. It may be configured to search a grid of model origins over a plausible volume to provide candidate model source time courses. Selection of a source with a peak SNR then provides a time course for the morphology validation and a model sphere location for the proximity validation.

The measure applied for the significance validation relies on a conservative estimate of the background interference in the average. Since the beamformer attenuates all external interference, the dominant interference for the investigated evoked response source location should be the leakage from sources of nearby spontaneous brain activity. It has been observed that fetal spontaneous brain signals may be up to ten times larger than the averaged evoked responses (Rose and Eswaran 2004), and the spatial filter is not sharp enough to provide sufficient attenuation. While the lower limit for the spontaneous burst characteristic frequency may be around 1 Hz, the period of the burst envelope is on the order of 5-20 s and is not stationary (Stockard-Pope *et al* 1992) so that it is unlikely to reliably capture this interference in the pre-stimulus window. In this work we have replaced the pre-stimulus background estimate with one based on a set of randomly triggered average values. This should conservatively

represent the average of all activity not time locked to the stimulus trigger (McCubbin *el al* 2007b).

Details of the data collection and processing method are presented in the next section. Validation of the method is then provided by processing data collected from a newborn baby on the fMEG array. In this example with good SNR and a well-known head position, OP processing, standard beamformer source reconstruction and a beamformer model search all produce similar results. Results from the fetal study are then discussed and the representative data are presented. We conclude that the flash-evoked response has been validated.

2. Materials and methods

The data consisted of 27 records from a flash-evoked fMEG study using a 151 channel MEG array conforming to a pregnant abdomen (CTF Systems, Vancouver). Subjects with normal pregnancies were recruited with informed consent and the protocol was approved by the institutional review board. The gestational age was between 30 and 36 weeks. Visual stimulation was provided by a 3.4 m fiber optic cable terminated in a 3 x 5 cm^2 woven panel (StockerYale, Salem). The input end of the cable was illuminated by four high-power LED arrays resulting in a light output of 35 mW at 630 nm (red) at the panel.

Three small (approximately 1 cm diameter by 3 mm thick) localization coils were positioned on the maternal hips and spine by means of an elastic belt for registration. The position and orientation of the fetus relative to the maternal abdomen was established by an ultrasound exam just before the MEG measurement. There was no co-registration of the ultrasound image with the MEG coordinate system, however the fetal eye position was roughly marked on the abdominal surface. This was used as a guide for the placement of the stimulator light panel. A fourth localization coil was attached to the light panel for registration.

The inter-stimulus interval (ISI) for this paradigm was 3.5 ± 0.5 s and the stimulus duration was 500 ms. Approximately 150 trials were collected at a sample rate of 312.5 Hz over a measurement session of 8 min. The data were filtered to a bandwidth of 0.5-10 Hz and trials were averaged over a time window of (-0.5, 1.5) s relative to the stimulus trigger after exclusion of trials from the average based on fetal movement, inferred from changes in fetal QRS p-p variations (actogram) (Zhao and Wakai 2002).

The fourth coil location was not reliable enough to establish the beamformer model search limits in the vicinity of the fetal head. As an alternative, the beamformer model origin search was conducted in two steps: once over approximately the entire maternal abdominal volume to estimate the fetal heart (fMCG) location and again over a smaller volume constrained by the knowledge of the fetal heart location, fetal head-heart orientation and the measurement geometry. The model used for both fMCG and fMEG searches was a single current dipole in a conducting sphere. The beamformer computation requires the forward solution based on the model, covariance matrix of the data and coordinates of both the origin and source search grids.

Covariance for the fMCG search was computed in a bandwidth of 0 to 70 Hz using all data in the record. A rectangular grid with limits of {(-17, 17), (-20, 15), (-30, -15)} cm in rectangular coordinates of the sensor array with an increment of 2 cm was established for the model origin search to cover most of the maternal abdominal volume. A spherical shell grid with radial limits of (2.5, 6.5) cm and an increment of 1 cm was used to construct beamformer source weights for each model origin. The source grid limits were established by visually optimizing the fMCG source time course resolution on a few example datasets. An average window of (-0.1, 0.4) s relative to fMCG QRS markers (determined by template matching), with a bandwidth of 0-70 Hz, was used to form an averaged fMCG time course over MEG channels. The MEG channel data were then transformed by beamformer weights to candidate

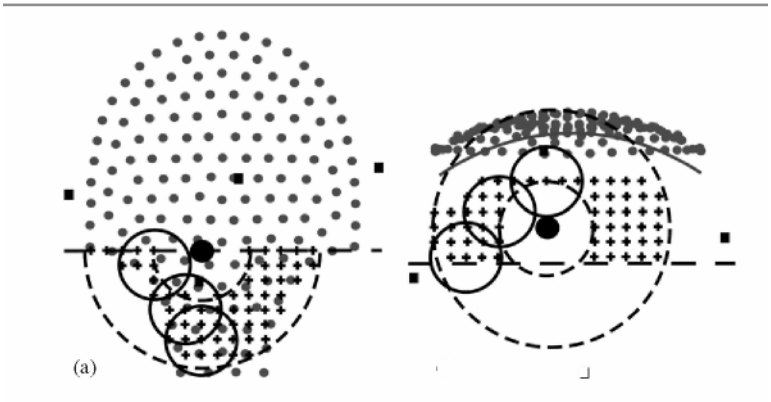

Figure 1. Example of model origin search for vertex orientation; grid slices through the fMCG origin ('+',2 cm spacing) superimposed onto sensor array projection (gray dots) with an estimated fMCG source location (large filled circle, r = 1.5 cm), three candidate model spheres (large open circles, r = 4.5 cm) and abdominal localization coils (filled squares). The dashed concentric circles (r = 6 and 15 cm) define the annular shell about the heart center for grid constraint: (a) projection onto the *x—y* plane; the horizontal dashed line limits the grid to head origins below the heart in this example, (b) projection onto the *x—z* plane; the horizontal dashed line limits the grid depth (4.5 cm deeper than the MCG center). The gray arc estimates the inner maternal abdominal surface (3 cm from the sensor coils).

source time courses for each origin/source grid location. The source location with the largest SNR was taken as a rough estimate of the fetal heart position (Robinson and Vrba 2004).

For the fMEG search, the covariance was computed in a bandwidth of 0.5 to 10 Hz and again in 0-70 Hz using all data remaining in the record after elimination of segments with fetal movement. The narrow band covariance was used to determine the beamformer model source orientation and the broadband covariance was used to compute the beamformer weights. The narrow band covariance was necessary to obtain a solution specifically for the expected frequency range of the evoked response while the broadband covariance provided weights which were valid over the full bandwidth of the recorded data. The usual rectangular grid model search over the entire maternal abdominal volume results in an ambiguity region of possible model origins due to the low SNR (Vrba *et al* 2007) and any beamformer model within this region can explain the data adequately. We have attempted to address this situation by limiting the search grid to geometrically plausible head model origins based on our estimate of the fetal heart location and fetal orientation from the ultrasound exam (either vertex—head down or breech—head up). A grid increment of 2 cm was used. An example origin search grid is shown in figure 1. A minimum heart radius of 1.5 cm and a fetal head radius of 4.5 cm were used to limit the closest possible head-heart origin distance to 6 cm. A maximum head-heart origin distance was estimated as the minimum plus one head diameter, or 15 cm. A maximum origin depth was set as one head radius below the fetal heart. Then for vertex (breech) orientation identified by a US exam just before the MEG session, the head must be below (above) the heart so we have taken only grid points below (above) the heart center, longitudinally. Origins which produced interference between a fetal head model radius of 4.5 cm and the maternal inner abdominal surface (with an estimated abdominal thickness of 1 cm) were excluded as well as origins outside the plan projection of the sensor array. At each origin a spherical shell with radii of 2 cm and 4.5 cm was used to limit the source search grid, with an increment of 1 cm.

The data were then averaged over a discrete time window of $(r., r+)$ = (-156, 469) samples or (-0.5, 1.5) s relative to the set of stimulus triggers, $(ts(i)\}$, $i = I,..., N$. The data were averaged again relative to / = 30 sets of randomized triggers, IR ($IR = t\$ \pm t_r$, t_r =

625 samples or 2 s with an exclusion of $\pm t_e$ = 188 samples or 0.6 s around each true stimulus trigger).

$$t_R(i, j) = R_j[\{t_S(i) - t_r, \ldots, t_S(i) - t_e\}, \quad \{t_S(i) + t_e, \ldots, t_S(i) + t_r\}], \quad i = 1, \ldots, N \quad \text{and} \quad j = 1, \ldots, J \tag{1}$$

where *Rj[-]* represents the operation of making a single random selection from the set of sample numbers indicated in the brackets. The averaged time course signal space vectors for

$$\mathbf{M}_j(\tau) = \frac{1}{N} \sum_{i=1}^{N} \mathbf{X}(t_R(i, j) + \tau), \quad \tau \in [\tau_-, \tau_+] \quad \text{and} \quad j = 1, \ldots, J \tag{2}$$

and the averaged time course signal space vector for the true triggers is

$$\mathbf{M}_0(\tau) = \frac{1}{N} \sum_{i=1}^{N} \mathbf{X}(t_S(i) + \tau), \quad \tau \in [\tau_-, \tau_+], \tag{3}$$

the randomized triggers are

where X(r) is the signal space vector at the time sample *t.* The baseline was subtracted based on the pre-trigger interval before projection of all / + 1 time courses through beamformer weights corresponding to every origin/source from the grid combination. Transforming from MEG signal space to a beamformer source space, the time course corresponding to the model origin index, *k,* and source index, 1, is given as

$$b_{jkl}(\tau) = \mathbf{W}_{kl} \cdot \mathbf{M}_j(\tau), \quad \tau \in [\tau_-, \tau_+], \quad j = 0, \ldots, J, \tag{4}$$

where W« is the beamformer weight vector for (model origin index, source index) = *(k, I).*

We have taken the set of randomized averages for a specific source as a sample of background noise in the averaged time course. Since the randomized triggers have no meaningful temporal relationship with the averaged time course points, the time points from all randomized averages were pooled and taken together as a random sample from the statistical distribution of the background noise. Compute the variance of the pooled randomized beamformer source values as

$$\sigma_{kl}^2 = \frac{1}{J + T - 1} \sum_{j,\tau} (b_{jkl}(\tau) - \mu_{kl})^2, \quad j = 1, \ldots, J, \quad \tau = \tau_-, \ldots, \tau_+, \tag{5}$$

where

$$\mu_{kl} = \frac{1}{J + T} \sum_{j,\tau} b_{jkl}(\tau), \quad j = 1, \ldots, J, \quad \tau = \tau_-, \ldots, \tau_+ \quad \text{and} \quad T = \tau_+ - \tau_- \tag{6}$$

and the summation is over all combinations of j and *T.* We have then tested the null hypothesis that a value equal to the peak of the true averaged evoked response time course may be drawn from the background distribution with a /7-value threshold of p = 0.001. Only sources for which this null hypothesis can be rejected were considered as candidate evoked response sources, i.e. we select all *(k, /)* such that

$$P\left[\operatorname{Max}_{\tau} |b_{0kl}(\tau)| G\left(0, \sigma_{kl}^2\right)\right] \leqslant p, \tag{7}$$

where *P[a, B]* is the probability of drawing the value 'a' from distribution '5' and *G* is the Gaussian distribution characterized by zero mean and variance of the pooled random sample.

An averaged time course signal to interference ratio was computed as

$$Q_{kl} = \left(\frac{1}{n_r} \sum_{t \in \Delta_r} b_{0kl}^2(t)\right)^{1/2} \left(\frac{1}{n_b} \sum_{t \in \Delta_b} b_{0kl}^2(t)\right)^{-1/2}, \tag{8}$$

where A_6 and A_r are the sets of time samples for background and response time windows relative to the stimulus trigger point and «_ is the number of samples in A_, so that Q_u is the rms ratio of the event-related signal to residual interference in the average. The background and response windows were taken as (-0.5, 0.1) s and (0.2, 0.8) s, respectively, assuming that a primary ER peak would occur no sooner than 100 ms after the trigger and no later than 800 ms after the trigger and further that the pre-trigger interval including 100 ms after the trigger should represent the averaged residual interference. It was expected that the ISI was long enough that there should be no response overlap from the preceding trial. Note that the pre- and post-intervals were of the same length to avoid bias.

Origin/source locations with/7 < 0.001 were then sorted by *Q* with the constraints such that the response rms should be greater than 5 nA m and less than 20 nA m to identify a few most plausible evoked response sources. Source locations with values of *Q* less than 2 were excluded because they generally did not satisfy the morphology criterion above. The amplitude constraints were imposed to avoid candidate sources that were unreasonably small or excessively large, possibly as a result of model mismatch, and the values were chosen experimentally. Finally the significance of event-related peaks was established by a 95% bootstrap confidence interval and related significance measure (McCubbin *et al* 2007b). The confidence intervals were plotted with the averaged response time coarse for a quick visual indication of response variability, however, the statistical significance of a post-trigger point in the average was quantified with an equal means test. The P-value of the observed post-trigger response was computed relative to the pooled random average background variance. A statistical power was determined from the overlap of the bootstrap distribution estimate with the background distribution estimate. We assigned statistical significance to a post-stimulus mean time point for/7 < 0.05 and power > 0.8.

An example recording from a newborn using the same apparatus and paradigm was used to validate the measurement protocol and the data processing method (except that the actogram trial rejection was not used). The newborn subject was positioned with the head near the center of the fMEG array and facing outward with head localization coils positioned above the nose and each ear. The flash stimulator light panel was mounted above the eyes at a distance of about 60 cm. A cradle-like attachment was used to support the newborn body.

The newborn data were first processed with a standard OP processing for comparison with an established event-related beamformer analysis (Robinson 2004, Cheyne *et al* 2007) using a single current dipole in a conducting sphere model. The origin of the model sphere was taken as the midpoint between localization coils positioned above the left and right ear. The background or control covariance was computed over the pre-stimulus interval and the signal or active covariance was computed over the post-stimulus interval (as defined above) in a 0 to 70 Hz bandwidth. The output of the processing was the ratio of the beamformer power in the active window to that in the control window for each point in a source grid within a spherical shell with an inner radius of 3.5 cm and an outer radius of 5.3 cm. The newborn data were then processed using the fMEG model search described above to validate the method used for the fetal data.

3. Results and discussion

The flash-evoked response of the example newborn subject is presented in figures 2 and 3. MEG channel time courses displayed in figure 2(a) were selected based on best *Q* after random average screening (the *Q* range over all channels was 8.6-1.9). A flat baseline with a broad peak between about 300 and 700 ms was observed with a maximum amplitude of about 55 fT. The data were processed with OP before averaging to attenuate interference from the newborn

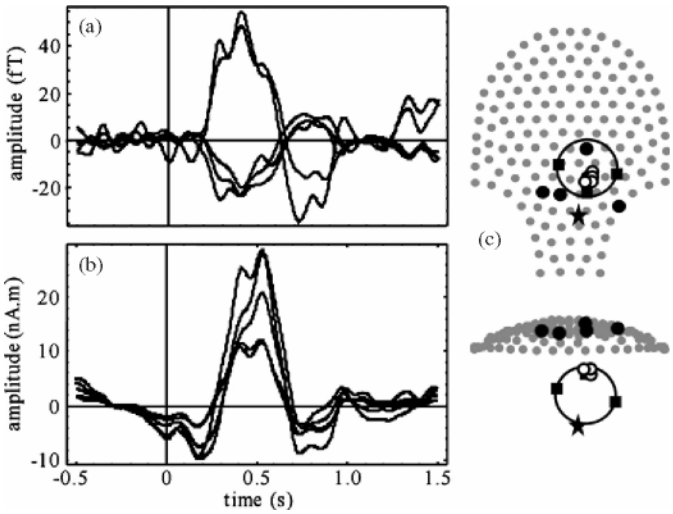

Figure 2. Example of newborn response to flash stimulation: (a) the five best OP processed MEG channel time courses (note the polarity reversal): Q = 8.6-7.1, (b) the five best beamformer source time courses, and (c) two projections of sensor array (gray dots) superimposed with head localization coil position (filled squares), estimated newborn heart location (star), selected MEG channel locations plotted in (a) (black dots), and the best few beamformer source locations plotted in (b) (small circles) with the head model (large circle).

heart. Signal redistribution due to OP explains the scatter in channel locations relative to the head position seen in figure 2(c) (Vrba *et al* 2004). The event-related beamformer processing resulted in a tight cluster of sources with a similar time course (figure 2(b)) as selected MEG channels and maximum amplitude near 30 nA m. The beamformer baseline was not as flat as the selected MEG channels, probably because the beamformer sources were selected based on the maximum beamformer power ratio rather than Q, according to Robinson (2004). Nonetheless both methods produce convincing evidence of an evoked response to the light flash stimulation paradigm, similar to the reported neonate responses (Huotilainen 2006).

The time course of the best few sources from the model search processing based on Q plotted in figure 3(a) has a very similar character to figure 2(a) but with a visibly improved SNR (the Q range over the five best was 21.9-19.6). The traces have been normalized and polarity matched by the peak value for ease of response shape comparison. The peak source amplitude varied between 3.4 and 7.5 nA m; much smaller than those of figure 2(b). This discrepancy may be due to the beamformer response to model inaccuracies. The best model sphere origins were spread by about one head radius around the true head model. The associated source locations had a similar scatter; consistent with the model search ambiguity behavior described in Vrba *et al* (2007). These results provide a clear validation of the model search method. The best source (based on Q) is plotted in figure 3(b) together with a 95% confidence interval and statistically significant time segments. The SNR for these data is good and the significance analysis is not really necessary for the validation of the newborn response, however it is provided for comparison with fetal results to follow. The significance at the end of the average window may be evidence of a very late response component or it could be a reminder that a 95% confidence interval is not a very strict condition.

A significant post-stimulus peak between about 180 and 770 ms latency was identified on 25 of 27 fetal records. Q varied from the minimum cutoff value of 2 to about 8, distributed as

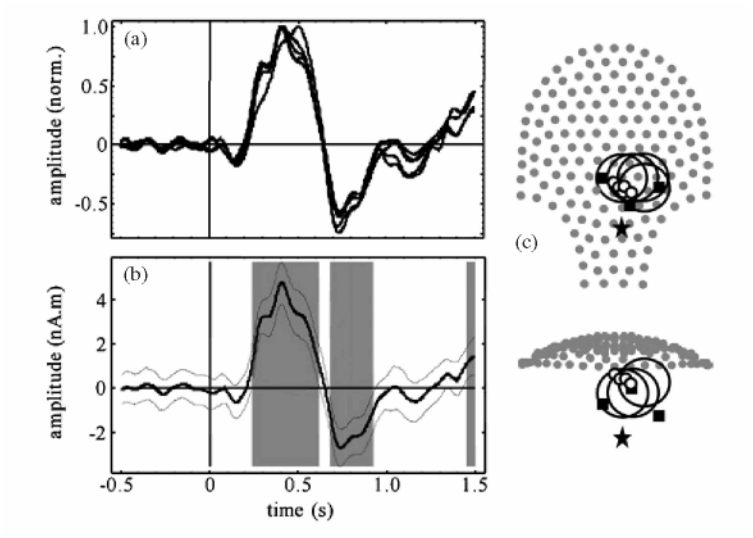

Figure 3. Model search processing of a newborn response example: (a) the five best source time courses, normalized and polarity matched by the peak value, (b) the time course of the best source (thick line) with a 95% confidence interval (thin lines) and statistically significant time segments (gray bands), and (c) two projections of a sensor array (gray dots) superimposed with a head localization coil position (filled squares), estimated newborn heart location (star), and the best few beamformer source locations (small circles) with the associated head models (large circles).

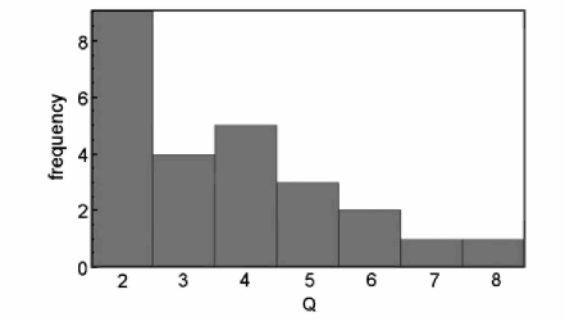

Figure 4. Histogram of Q for 25 datasets.

shown in the histogram of figure 4. The histogram indicates the limited global robustness of the response with a Q below 3 for one third of the records. The peak source amplitude was between about 4 and 40 nA m. The response latency was measured as the first significant peak or shoulder. There was a hint of latency reduction with increasing GA, but the variance was too large to make any conclusion, especially at 33 and 36 weeks. This approach has an inherent limitation, because latencies of different component complexes describing the morphology of a visual evoked response can be intermixed. In a recent paper (Eswaran *et al* 2004) we used a simple separation scheme of the evoked components to investigate early (<300 ms) and late responses (>300 ms). The latency of the early response showed a significant decrease with gestation. In the current study this approach was not applicable, because only six recordings showed a significant response with a latency below 300 ms.

The three fetal records with the largest Q are presented in figures 5(a)-(c). The SNR was low even for these exemplary records, as seen in the significance plots of the best source time

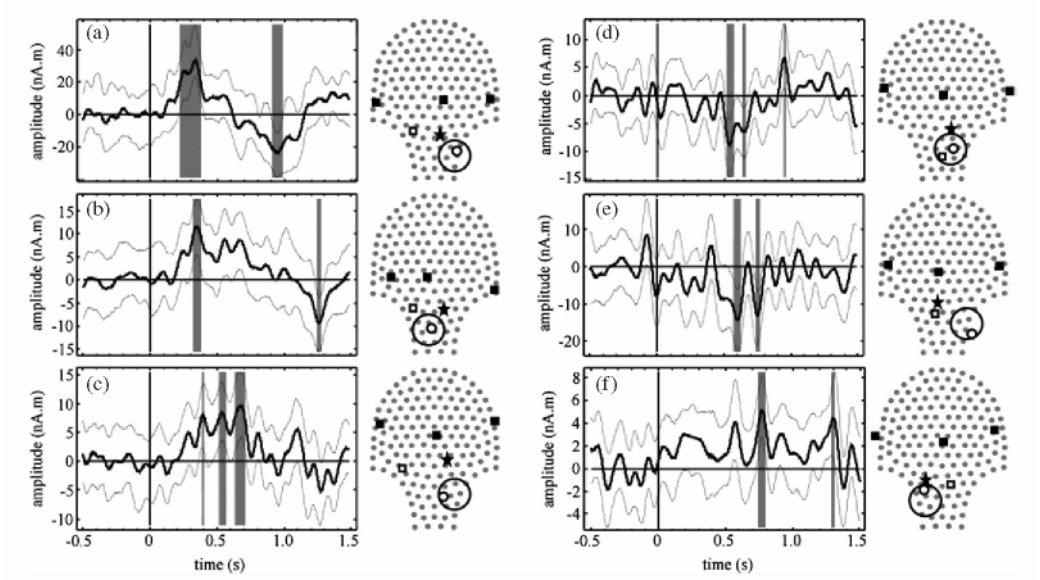

Figure 5. Model search results from fetal response to flash stimulation for each of the three best SNR datasets (a)-(c) and the poorest three SNR datasets (d)-(f). For each example, left: time course of the one best source (thick line) with 95% confidence interval (thin lines) and statistically significant time segments (gray bands); right: projection of a sensor array (gray dots) superimposed with localization coil positions (filled squares), fourth coil position (open square), estimated fetal heart location (star) and the best source location (small circle) with a head model (large circle).

course for each example; however a clear response peak was readily identified. The selected head models were consistent with ultrasound exam notes, however the proximity to the fourth coil was large in some cases. The method of attaching the localization coil to the light panel was not secure and the coil tended to slip from its intended position as the subject's abdomen was engaged with the sensor array surface and might explain the observation. On the other hand, the distance between the fourth coil and head model origin could be expected to be up to about 18 cm given the model origin ambiguity of about 1 head diameter, the head radius and an additional 3 to 5 cm to account for the fetal head surface to abdominal wall distance. The maximum fourth coil to the origin distance observed was 18.4 cm, with 15 of 25 records less than 11 cm, and 23 of 25 less than 18 cm. As such, even though there was no clear discrepancy, the fourth coil position was not used as a component of the validation due to the limited resolution.

The three fetal records with the smallest Q are presented in figures 5(d)-(f) for contrast. In these cases, it was difficult to see an evoked response above the background signal by eye, however a significant peak was still detected for the best source in each case. The time course of figure 5(e) had a poor baseline and that of figure 5(f) was a borderline case where only two sources passed the random average screening and the significant peak was rather late, at 770 ms (possibly due to the offset of the stimulus at 500 ms).

4. Conclusions

We have demonstrated three criteria for validation of the averaged flash-evoked response of the fetus (statistical significance of the time course, proximity of significant modeled source to the estimated fetal head location and observation of physiologically plausible time

course morphology) for 25 of a sample of 27 subjects with a gestational age between 30 and 36 weeks. The environmental and biomagnetic interference was suppressed by using a beamformer model search over a plausible abdominal volume based on geometrical constraints including proximity to the fetal heart. A statistical screening was employed to limit the false detection of an evoked response by the chance average of residual interference; estimating a background distribution from a set of randomized averages and testing the null hypothesis that a candidate response could be drawn from that background distribution. The screened source with the largest SNR time course was then accepted as the most plausible model and the response latency was estimated from the earliest statistically significant post-stimulus peak.

The response time course and the associated latency were quite variable and it was not possible to demonstrate the expected decrease in latency with increasing gestational age. Perhaps SNR is still insufficient and additional processing refinements may be required. Alternatively, the large variability in the EEG-evoked response latency of premature newborns (Umezaki and Morrell 1970) suggests that we may be able to demonstrate the correlation with a larger sample size. Further studies are needed to develop a refined classification scheme for visual evoked fields in the fetus. We also intend to apply this processing method to auditory paradigms and to test other neurophysiological processes such as habituation.

The search grids were determined with rough estimates for physiological dimensions. An improved procedure would be to use ultrasound/MEG co-registration or at least individual anthropomorphic data from the ultrasound exam for beamformer search grid constraints and head model size. It is also recognized that the heart model is poor but both these limitations were deemed adequate and within the required precision given the ambiguity. Future work will include the development of a method for co-registration of 3D ultrasound fetal head images with MEG. We also intend to improve the reliability of the ultrasound-guided placement of the fourth localization coil so that a 3D ultrasound procedure may not be routinely necessary.

Acknowledgements

The work was supported by the US National Institutes of Health under grants 1R01NS367704A1 and 1R33EB00978-01.

References

Cheyne D, Boston A C, Gaetz W and Pang E W 2007 Event-related beamforming: a robust method for presurgical functional mapping using MEG *Clin. Neurophysiol.* **118** 1691-704 Eswaran H, Lowery C L, Wilson J D, Murphy P and Preissl H 2004 Functional development of the visual system in human fetus using magnetoencephalography *Exp. Neurol.* **190** S52-8 Eswaran H, Wilson J D, Preissl H, Robinson S E, Vrba J, Murphy P, Rose D F and Lowery C L 2002 Magnetoencephalographic recordings of visual evoked brain activity in the human fetus *The Lancet* 360 779-80

Huotilainen M 2006 Magnetoencephalography of the newborn brain *Semin. Fetal Neonatal Med.* **11** 437-43

McCubbin J, Murphy P, Wilson J D, Eswaran H, Preissl H, Robinson S E, Yee T, Vrba J and Lowery C L 2007a Improved flash evoked response from fetal MEG *Int. Congr. Ser.* **1300** 749-52 McCubbin J, Robinson S E, Cropp R, Moiseev A, Vrba J, Murphy P, Priessl H and Eswaran H 2006 Optimal reduction of MCG in fetal MEG recordings *IEEE Trans. Biomed. Eng.* 53 1720-4 McCubbin J, Yee T, Vrba J, Robinson S E, Murphy P, Eswaran H and Preissl H 2007b Bootstrap significance of low SNR evoked response /. *Neurosci. Methods* submitted

Robinson S E 2004 Localization of event-related activity by SAM(erf) *Neurol. Clin. Neurophysiol.* **2004** 109

Robinson S E and Vrba J 2004 Cleaning fetal MEG using a beamformer search for the optimal forward model *Biomag 2004* (Boston, MA, USA) ed E Halgren *et al* pp 339-40

Rose D F and Eswaran H 2004 Spontaneous neuronal activity in fetuses and newborns *Exp. Neurol.* **190** S28-36

Stockard-Pope J E, Werner S S and Bickford R G 1992 *Atlas of Neonatal Electroencephalography* (New York: Raven Press) pp 105-75

Umezaki H and Morrell F 1970 Developmental study of photic evoked responses in premature infants *Electroenceph. din. Neurophysiol.* 28 55-63 Vrba J, Robinson S E, McCubbin J, Lowery C L, Eswaran H, Murphy P and Preissl H 2007 Searching for the best model: ambiguity of inverse solutions and application to fetal magnetoencephalography *Phys. Med. B iol.52757-7 6* Vrba J, Robinson S E, McCubbin J, Lowery C L, Eswaran H, Wilson J D, Murphy P and Preissl H 2004 Fetal MEG redistribution by projection operators *IEEE Trans. Biomed. Eng.* **51** 1207-18 Zhao H and Wakai R T 2002 Simultaneity of foetal heart rate acceleration and foetal trunk movement determined by foetal magnetocardiogram actocardiography *Phys. Med. Biol.* 47 839-46